ARID ZONE JOURNAL OF ENGINEERING, TECHNOLOGY & ENVIRONMENT
AZOJETE June 2026. Vol.22(2):502-512
Published by the Faculty of Engineering, University of Maiduguri, Maiduguri, Nigeria.
Print ISSN: 1596-2490, Electronic ISSN: 2545-5818
https://doi.org/10.63958/AZOJETE/2026/22/02/027
www.azojete.com.ng

ORIGINAL RESEARCH ARTICLE

EXPERIMENTAL PERFORMANCE EVALUATION OF A SOLAR AIR HEATER USING RECYCLED ALUMINUM SODA CANS ABSORBERS UNDER MAIDUGURI CLIMATIC CONDITIONS

B. G. Jidda*, S. Shodiya, S. A. Abdulrahman

Department of Mechanical Engineering, University of Maiduguri, Maiduguri, Nigeria
**Corresponding author's email: babajidda124@gmail.com*

ARTICLE INFORMATION

Received: 18th April 2026
Revised: 10th May 2026
Accepted: 16th May 2026

Keywords:
Solar air heater
Recycled aluminium cans
Forced convection
Natural convection
Thermal efficiency
Renewable energy
Maiduguri climate

ABSTRACT

This study experimentally investigated the performance of a solar air heater (SAH) constructed using recycled aluminium beverage soda cans as absorber tubes under Maiduguri harmattan climatic season. The research addressed the growing need for low-cost, environmentally sustainable heating systems for applications such as space heating and crop drying in regions with abundant solar radiation. The system was designed as a single-pass solar air collector with dimensions 1.09 m × 0.835 m × 0.15 m and collector area of 0.91 m². The absorber consisted of 96 aluminium soda cans arranged in a 12 × 8 matrix and coated with black paint to improve solar absorptivity. Experiments were conducted in active mode using a 12 V DC fan with air mass flow rate of 0.00113 kg/s and in passive mode airflow movement which occurred naturally through buoyancy-driven convection. The collector was tested at tilt angles of 25°, 30°, 45°, 60°, and 180°. Performance parameters included outlet air temperature, temperature rise, useful heat gain, and collector efficiency. Results indicated that the active system achieved a maximum thermal efficiency of 14 % with useful heat gain of approximately 90W at 45° tilt angle. Also, the passive mode achieved 16% efficiency with optimum performance at 45° tilt angle with maximum useful heat gain of 130.2W. The results confirmed that discarded aluminium cans can be effectively used as low-cost absorber materials for solar air heaters in solar-rich regions, such as Maiduguri.

1.0 Introduction

The escalating prices of fossil fuels and growing environmental concerns have renewed global interest in alternative energy resources. Solar energy, being the most abundant renewable energy source, offers tremendous potential for both electricity generation and direct thermal applications (Singh *et al.,* 2022).Solar air heaters (SAHs) are particularly attractive for agricultural crop drying, residential space heating, and small-scale industrial preheating processes due to their simple design, low maintenance requirements, and use of non-corrosive working fluids (Murali *et al.,* 2020).

Conventional SAHs typically employ flat-plate absorbers, metallic fins, or perforated plates to enhance heat transfer. However, the cost of high-quality absorber materials and fabrication can be prohibitive, especially in low-income or rural communities. This has motivated researchers to explore alternative low-cost absorber materials, including recycled waste materials. Aluminium soda cans present an innovative solution: they possess high thermal conductivity, lightweight, and are readily available as waste. When appropriately arranged, these cans can function as individual tube absorbers that enhance heat transfer and increase the effective surface area within the collector (Mgbemene *et al*., 2022).

The performance of SAHs depends not only on absorber material and geometry but also on the operational mode. Passive systems rely on natural convection driven by buoyancy forces, offering simplicity and zero parasitic energy consumption but limited airflow rates. Active systems employ fans or blowers to force air through the collector, increasing mass flow rates and enhancing useful heat gain, albeit with additional energy requirements (Prasad *et al,.*2017).

Abdulkarim (2020) investigated the effect of reflector on newly single pass solar air heater and concluded that there was improvement in thermal efficiency by 10 percent in solar air heater by using reflectors. Also the mass flow rate of the SAH was proportional to the efficiency. Likewise Mandal and Ghosh (2020) performed an experiment on solar air heater with a reflecting source and found the mass flow rate of air to be proportional to the efficiency. In an experimental study of Karoua *et al*., (2016) with Linear Fresnel reflector of solar air heater, the outlet temperature of air achieved was 150°C. Bhowmik and Amin (2017) proposed a technique to enhance the solar collector's performance. He used reflecting element with the solar collector to heat up the water.

Maiduguri, located in northeastern Nigeria (11.83°N, 13.15°E), experiences a hot semi-arid climate characterized by high solar irradiance (5.5–6.5 kWh/m²/day), making it ideal for solar thermal applications (Abdulkarim 2020). However, limited experimental data exist on the performance of low-cost SAHs using aluminium cans under Maiduguri-specific climatic conditions, particularly regarding comparative analysis of passive and active operational modes at various tilt angles.

This study aimed to experimentally evaluate the performance of a solar air heater with a tube-absorber fabricated from discarded aluminium soda cans under Maiduguri Hamattan weather conditions. The specific objectives were to: Design a tube absorber solar air heater using beverage soda cans, fabricate the designed solar air heater, test the heater in both active (forced convection) and passive (natural convection) modes at various tilt angles, and evaluate and compare thermal performance parameters including temperature rise, useful heat gain, and thermal efficiency.

Overall, this research contributed to sustainable energy practices by demonstrating the feasibility of recycled materials in solar thermal applications, potentially lowering construction costs and making renewable energy more accessible. The findings provided valuable design guidance for similar solar-rich regions and support waste reduction efforts through material recycling.

2. Materials and Method

2.1 Study Area

The experiment was carried out in Maiduguri, North-East Nigeria (11.83°N, 13.15°E), during the Harmattan season, which is characterized by high solar radiation levels of approximately 5.5–6.5 kWh/m²/day and average daytime temperatures ranging from 33 to 45 °C (Abdulkarim, 2020).

2.2 Solar Air Heater Design and Fabrication

The SAH was designed as a single-pass flat-plate collector with a tube-packed-bed absorber made of aluminium soda cans, following Guy Sperry's design guidelines for design calculation Sperry (2011). Table 1 and Table 2 shows collector specification and instrumentation respectively. While plate 1a and 1b show collector absorber tube configuration and completed installation of SAH component.

Table 1: Design and construction parameters of the solar air heater collector

Parameter	Value
Collector dimension	1.09 m × 0.835 m × 0.15 m
Aperture area	0.91 m^2
Glazing	4 mm glass ($\tau \approx 0.88$)
Absorber material	96 aluminium cans (330 ml)
Can arrangement	12 rows × 8 columns, staggered
Surface coating	Matt black paint ($\alpha \approx 0.95$)
Insulation	25 mm Styrofoam
Casing	12 mm plywood

Corresponding author's email address: babajidda124@gmail.com

Table 2: Measurement instruments and associated parameters used in the experimental

Instrument	Parameter	Accuracy
Digital thermometers	Inlet/outlet temperature	±0.1°C
Pyranometer	Solar irradiance	±5 W/m^2
Hot-wire anemometer	Air velocity	±0.1 m/s
Digital protractor	Tilt angle	±1°
Digital Spirit level	Collector orientation	

The instruments accuracies according to manufacturer specifications are shown in Table 2.

(a) (b)

Plate 1: Collector absorber tube (cans) configurations (a), completed installation of all SAH components (b)

2.3 Experimental Procedure

2.3.1 Test matrix

Two operational modes were investigated. Airflow movement occurred naturally through buoyancy-driven convection in passive mode (natural convection), and in active mode (forced convection) airflow was induced using a 12 VDC fan with a measured mass flow rate of 0.00113kg/s. The collector was tested at tilt angles of 25°, 30°, 45°, 60°, and 180° for both forced and natural convection, respectively. Temperature measurements were taken at the collector inlet and outlet while solar radiation was recorded simultaneously.

2.3.2 Experimental setup

The experimental setup was prepared by verifying the integrity of the insulation, the condition of the glazing, and the arrangement of the absorber, while proper sealing of the collector components was ensured to minimize heat losses. Thermometers were positioned at the inlet and outlet sections of the collector for temperature measurements, while the pyranometer was calibrated before the commencement of the experiment. The collector tilt angle was adjusted and verified using a digital protractor to ensure proper orientation toward solar radiation.

During passive testing, the system was allowed to attain natural airflow stabilization, and the inlet temperature, outlet temperature, and solar irradiance were recorded at 1-hour intervals between 09:00 and 14:00. For active testing, a DC fan was activated to induce forced convection airflow through the collector, and the airflow rate was verified before measurements were taken. The same operating parameters were recorded at identical time intervals throughout the active test period.

2.4 Theoretical Calculations

2.4.1 Useful heat gain (Q_u)

The useful heat gain was calculated using the energy balance equation (John Wiley *et al.,* 2013).

$$Q_u = \dot{m}\, C_p\, (T_{out} - T_{in}) \quad \text{I}$$

Corresponding author's email address: babajidda124@gmail.com

Where $\dot{m}$ = 0.00113 kg/s (active mode, measured), C_p= 1005 J/kg K (specific heat of air at constant pressure), T_{out} and T_{in} = outlet and inlet air temperatures (°C)

Passive mode mass flow rate:

$$\dot{m} = \rho VA \quad (2)$$

Where $\rho = \frac{1.13\text{kg}}{m^3}$, $A_c = 0.00096\, m^2 (duct\ area)$, $V = 2.2\, m/s$ (velocity of air), $\dot{m} = 0.0024 kg/s$

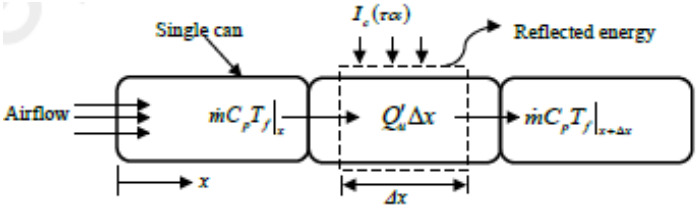

Figure 2: Determination of heat transfers property of air flows through connected soda cans

Figure 2 depicts how solar radiation transfers heat into the air flowing through the soda can. For passive mode, mass flow rate was estimated from buoyancy-driven flow correlations (Incropera *et al.,* 2013).

2.4.2 Thermal efficiency (η)

Kreith and Bohn (2004) said that collector thermal efficiency was determined as

$$\eta = {}^{Q_u}/_{I_c A_c} \times 10\% \quad (3)$$

where I_c = Solar irradiance (W/m^2), A_C= collector aperture area (0.91m^2)

3. Results and Discussion

3.1 Temperature Profiles at Different Tilt Angles for Active Mode

Figures 3–8 present the temperature profile at different tilt angle for active mode. This corresponds to the outlet air temperatures (T_{out}) and corresponding solar irradiance (I_c) results at various tilt angles. Figure 3 shows the active mode performance at 25° tilt. Outlet temperature increased from 75°C at 09:00 (639 W/m²) to a maximum of 106°C at 12:00 (942 W/m²), then decreased to 91°C by 14:00 (771 W/m²). The observed increase and subsequent decrease in outlet temperature was attributed to the variation in incident solar radiation, combined with increased thermal losses after peak heating conditions.

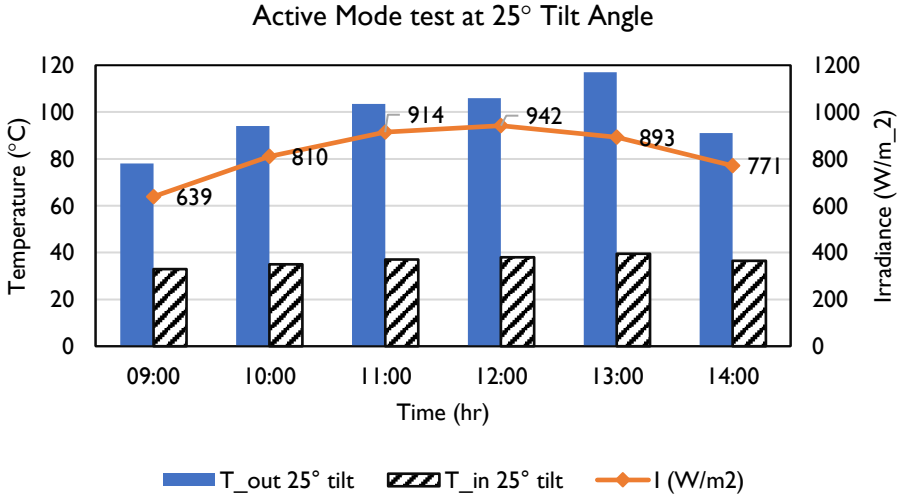

Figure 3: Solar Irradiance and outlet temperature at 25° tilt angle

Figure 4 presents result at 30° tilt. Temperatures ranged from 74°C at 09:00 (568 W/m²) to 108°C at 14:00 (783 W/m²), with 102.5°C recorded at 12:00 (942 W/m^2). The delayed peak temperature observed at 14:00

for the 30° tilt was attributed to improved solar incidence angle in the afternoon and thermal energy storage within the absorber plate, which outweigh the reduction in solar radiation intensity after midday.

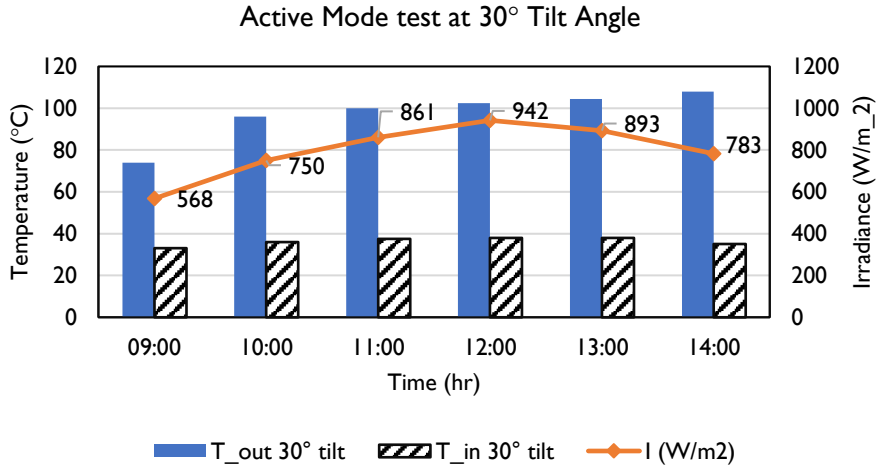

Figure 4: Solar Irradiance and outlet temperature at 30° tilt angle

Figure 5 illustrates performance at 45° tilt, which exhibited the highest overall temperatures. Outlet temperature reached 118°C at 12:00 (850 W/m²), with consistent performance throughout the testing period. The superior performance at 45° tilt was attributed to improved solar incidence angle, which enhances effective solar energy absorption. This results in higher useful heat gain and stable thermal performance, despite moderate solar radiation levels compared to lower tilt angles.

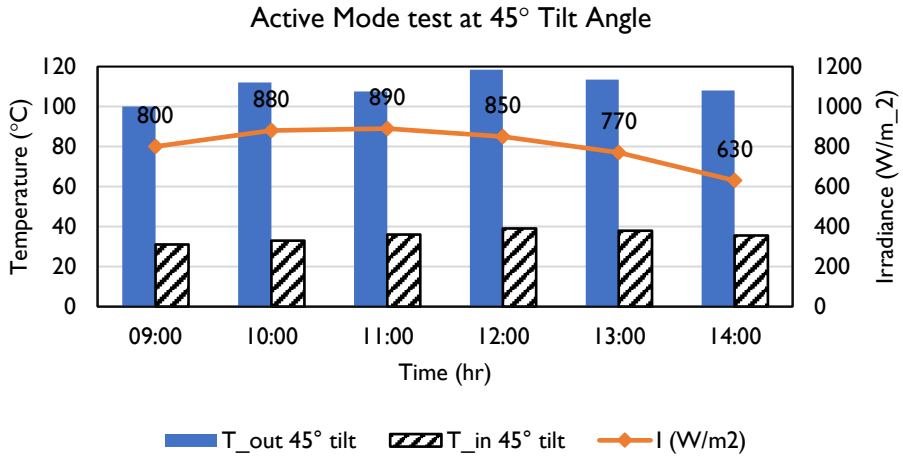

Figure 5: Solar Irradiance and outlet temperature at 45° tilt angle

Figure 6 shows results at 60° tilt, with temperatures ranging from 78°C at 09:00 (800 W/m^2) to 112°C at 14:00 (630 W/m^2). The delayed peak temperature at 60° tilt was attributed to suboptimal solar incidence at midday and improved alignment with solar rays in the afternoon, combined with thermal energy storage in the absorber plate, which enhances heat output despite reduced solar radiation intensity.

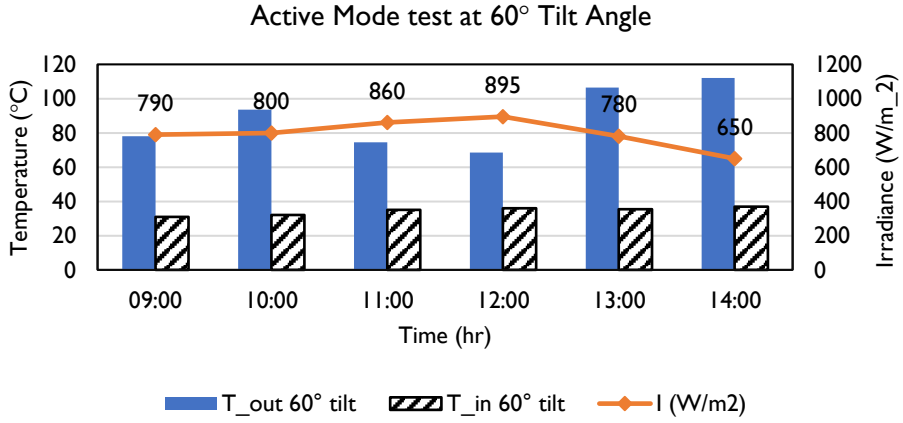

Figure 6: Solar Irradiance and outlet temperature at 60° tilt angle

Corresponding author's email address: babajidda124@gmail.com

Figure 7 presents performance at 180° (horizontal orientation), where temperatures varied from 71°C at 09:00 (562 W/m^2) to 104°C at 12:00 (763 W/m^2).

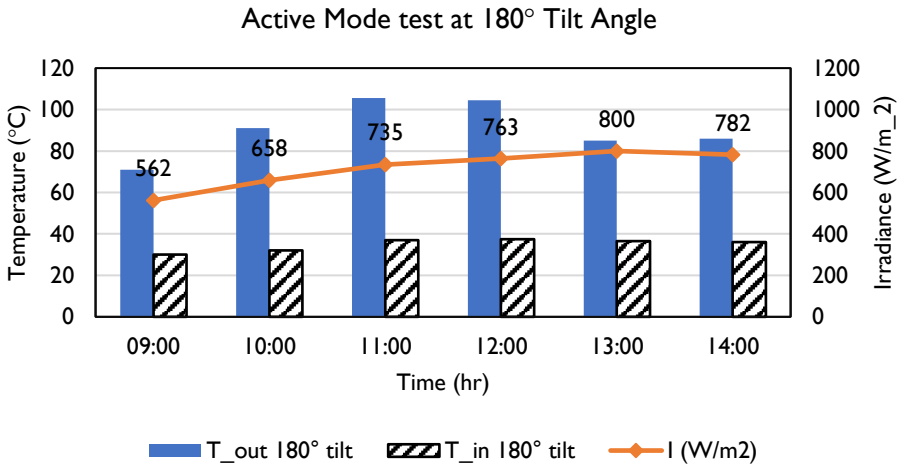

Figure 7: Solar Irradiance and outlet temperature at 180° tilt angle

3.2 Active Mode Performance at 45° (Optimal)

Table 3 summarizes the experimental data for active mode at the optimal tilt angle of 45°, from which performance was consistent throughout the testing period.

Table 3: Active Mode Experimental Data at 45° Tilt (Optimal)

Time	I (W/m^2)	T_in (°C)	T_out (°C)	ΔT (°C)	Q_u (W)	η (%)
09:00	800	31.0	100.0	69.0	78.36	10
10:00	880	33.5	112.0	78.5	89.15	11
11:00	890	36.0	107.5	71.5	81.19	10
12:00	850	39.0	118.0	79.5	90.28	11
13:00	770	38.0	113.5	75.5	85.74	12
14:00	630	35.5	108.0	72.5	82.33	14

The maximum temperature rise (ΔT = 80°C approx.) occurred at 12:00, coinciding with peak solar irradiance. Thermal efficiency ranged from 10 to 14%, with the highest efficiency recorded at 14:00 despite lower irradiance, suggesting reduced thermal losses during afternoon hours.

3.3 Temperature Profiles at Different Tilt Angles for passive Mode

Figures 8–13 present the outlet air temperatures and corresponding solar irradiance for passive mode tests at various tilt angles. Figure 8 shows the passive mode performance at 25° tilt. Outlet temperature increased from 48°C at 09:00 (639 W/m²) to a maximum of 75°C at 12:00 (892 W/m²), then decreased to 67°C by 14:00 (723 W/m²). The observed trend is attributed to the variation in solar irradiance and solar incidence angle throughout the day. The increase in outlet temperature from morning to noon is due to rising solar radiation and enhanced buoyancy-driven airflow, while the subsequent decrease in the afternoon results from reduced irradiance and increased thermal losses.

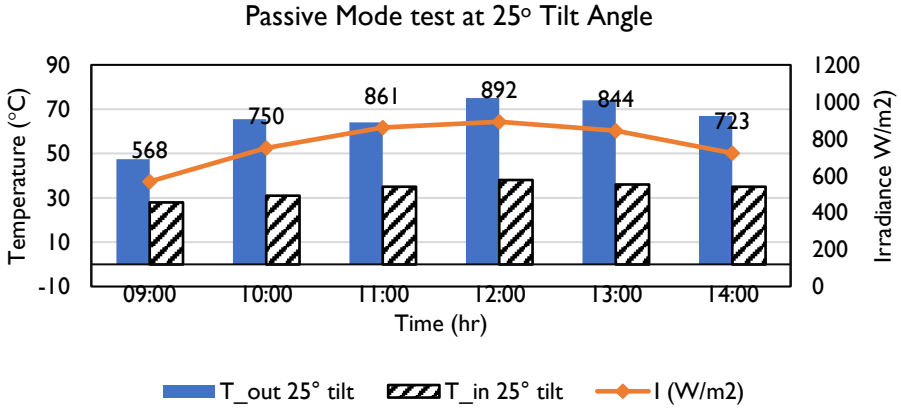

Figure 8: Solar Irradiance and outlet temperature at 25° tilt angle

Corresponding author's email address: babajidda124@gmail.com

Figure 9 shows the passive mode performance at 30° tilt. Outlet temperature increased from 54 °C at 09:00 (570 W/m^2) to a maximum of 78 °C at 12:00 (825 W/m^2), then decreased to 66 °C by 14:00 (723 W/m^2). The temperature trend at 30° tilt is governed by the variation in solar irradiance and buoyancy-driven airflow. The increase from morning to noon is due to rising solar radiation and improved heat absorption, resulting in higher outlet temperatures. The decrease in the afternoon is attributed to declining irradiance, reduced incidence angle efficiency, and increased thermal losses to the environment.

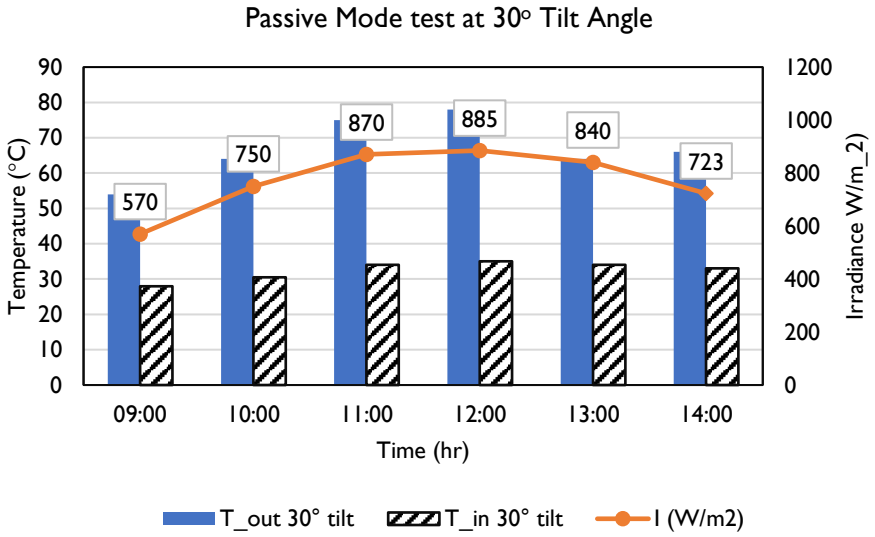

Figure 9: Solar Irradiance and outlet temperature at 30° tilt angle

The result of the passive mode test of the SAH at 45° tilt presented in Figure 10 was the optimal performance. The outlet temperatures increased from 59 °C at 09:00 (780 W/m^2) to 89 °C at 12:00 (915 W/m^2), then decreased to 76 °C by 14:00 (760 W/m^2). The superior performance at 45° tilt is attributed to improved alignment with solar radiation, which enhances incident energy absorption and reduces reflection losses. The rise in outlet temperature from morning to noon was due to increasing solar irradiance and intensified buoyancy-driven airflow. The subsequent decline in the afternoon results from reduced irradiance, suboptimal solar incidence, and increased thermal losses to the surroundings.

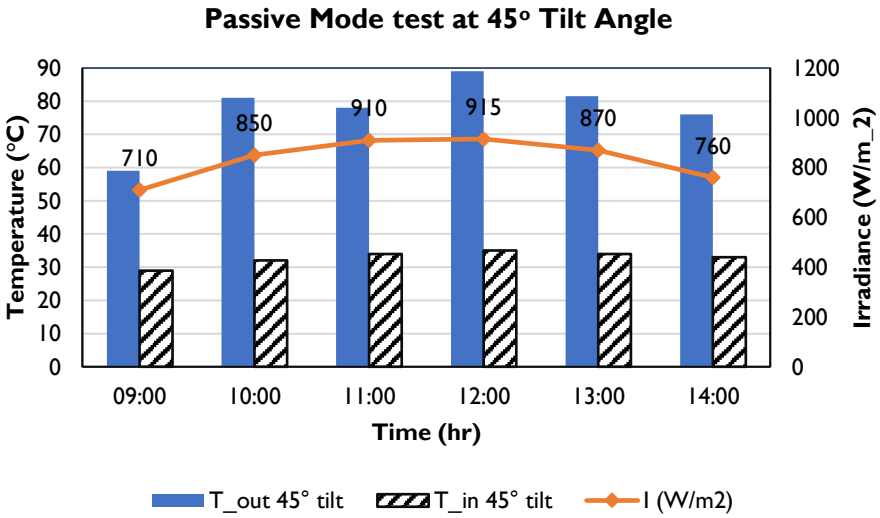

Figure 10: Solar Irradiance and outlet temperature at 45° tilt angle

Figure 11 shows the passive mode performance at 60° tilt. Outlet temperature increased from 74 °C at 09:00 (780 W/m^2) to a maximum of 89 °C at 12:00 (960 W/m^2), then decreased to 76 °C by 14:00 (870 W/m^2), the observed trend at 60° tilt is influenced by solar incidence angle and thermal losses. The relatively high morning temperature is due to better alignment with low solar angles, enhancing early heat absorption. The increase to peak temperature at noon is driven by maximum solar irradiance despite suboptimal tilt alignment. The subsequent decrease in the afternoon is attributed to reduced incidence efficiency and increased convective heat losses associated with the steep collector angle.

Corresponding author's email address: babajidda124@gmail.com

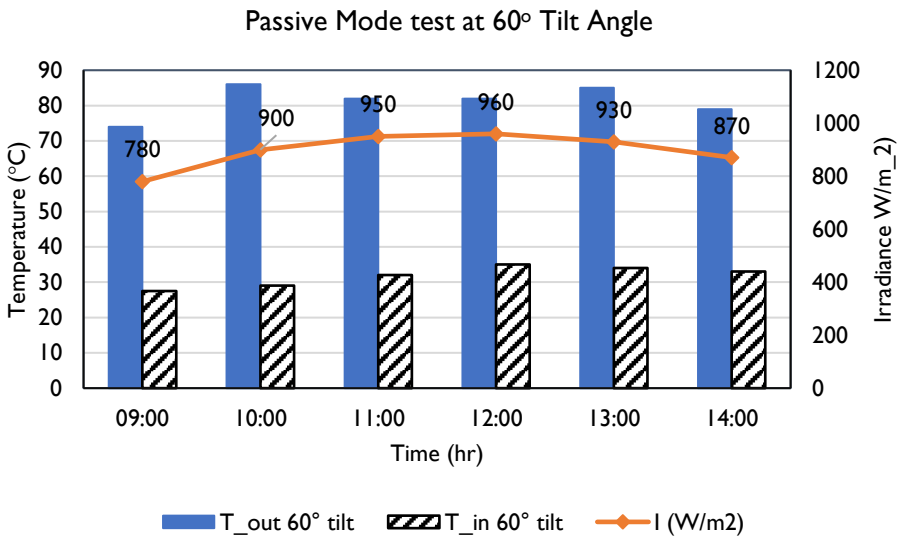

Figure 11: Solar Irradiance and outlet temperature at 60° tilt angle.

Figure 12 shows the passive mode performance at 180° tilt. Outlet temperature increased from 53 $°C$ at 09:00 (780 W/m^2) to peak values between 70 - 72 $°C$ by 11:00-12:00. However, as the irradiance decreases from 1030 W/m^2, the outlet temperature increases to 73 $°C$ by 14:00 (880 W/m^2). The anomalous trend at 180° tilt was attributed to the ineffective orientation of the collector with respect to solar radiation, resulting in minimal direct energy absorption and reliance on diffuse and reflected radiation. The gradual increase in temperature from morning to midday was due to limited heat gain, while the continued rise in outlet temperature in the afternoon, despite decreasing irradiance, was caused by thermal storage and delayed heat release within the system under low airflow (passive) conditions.

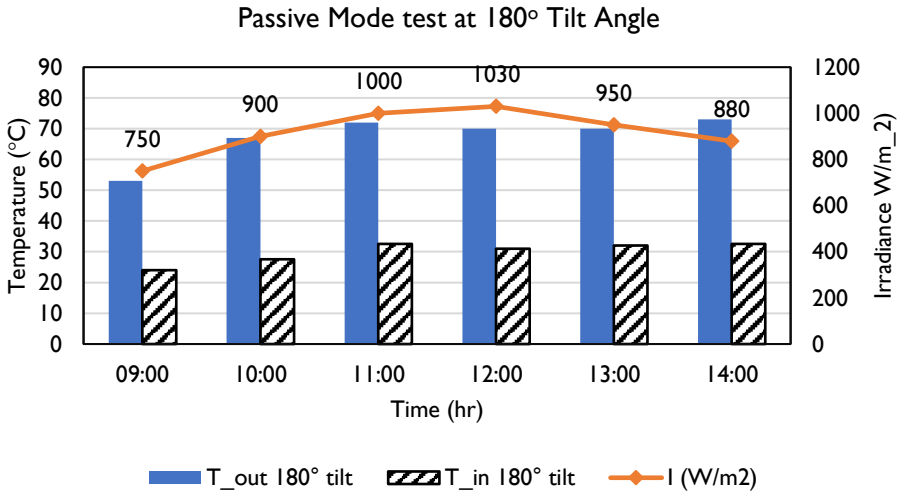

Figure 12: Solar Irradiance and outlet temperature at 180° tilt angle

3.4 Passive mode Performance at optimal tilt Angle

The optimal performance for passive mode was also obtained at 45°. Table 4 summarizes the experimental data obtained, from which performance was consistent throughout the testing period.

Table 4: Passive Mode Experimental Data at 45° Tilt (Optimal)

Time	I (W/m²)	T_in (°C)	T_out (°C)	ΔT (°C)	Q_u (W)	η (%)
09:00	710	29	59.0	30.0	72.36	11.2
10:00	850	32	81.0	49.0	118.19	15.3
11:00	910	34	78.0	44.0	106.13	12.8
12:00	915	35	89.0	54.0	130.25	16.0
13:00	870	34	81.5	47.5	114.57	14.5
14:00	760	33	76.0	43.0	103.72	15.0

Corresponding author's email address: babajidda124@gmail.com

The 45° tilt angle yielded the highest performance with ΔT = 54 °C and efficiency of 16%, despite not receiving the highest solar irradiance. This indicates optimal orientation for both solar capture and buoyancy-driven airflow at Maiduguri's latitude.

3.5 Performance Analysis of SAH

3.5.1 Effect of tilt angle on temperature rise (ΔT)

Temperature rise (ΔT) of the system for both active and passive mode obtained are compared at different tilt angles. ΔT is the temperature difference between the T_{in} and T_{out} from the absorber collector area. Figure 13 shows the profile of the temperature distribution.

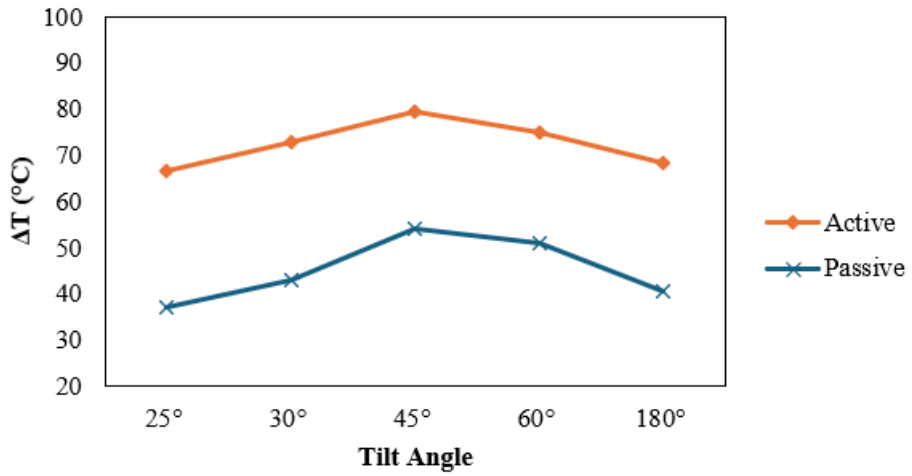

Figure 13: Temperature rise (ΔT) for active and passive mode at different SAH tilt angles

Temperature rise (ΔT) for both active and passive modes at their respective optimal configurations, i.e. when T_out is maximum were used. Active mode maintained consistently higher ΔT values (67–75°C) compared to passive mode (37–54°C). The enhanced performance in active mode was attributable to improved heat transfer coefficient between absorber surface and air stream.

3.5.2 Effect of tilt angle on useful heat gain

Figure 14 and 15 presents useful heat gain and thermal efficiency of the SAH for both operating modes. Thermal efficiency for passive mode (11–16%) significantly exceeded active mode values (9–14%). The useful heat gain for active mode peaked at 60° tilt (85.2 W) and ranged from 76 W to 85.2 W. Passive mode achieved maximum useful heat gain of 130.2 W at 45° tilt angle, representing a 34.6% increase compared to active mode.

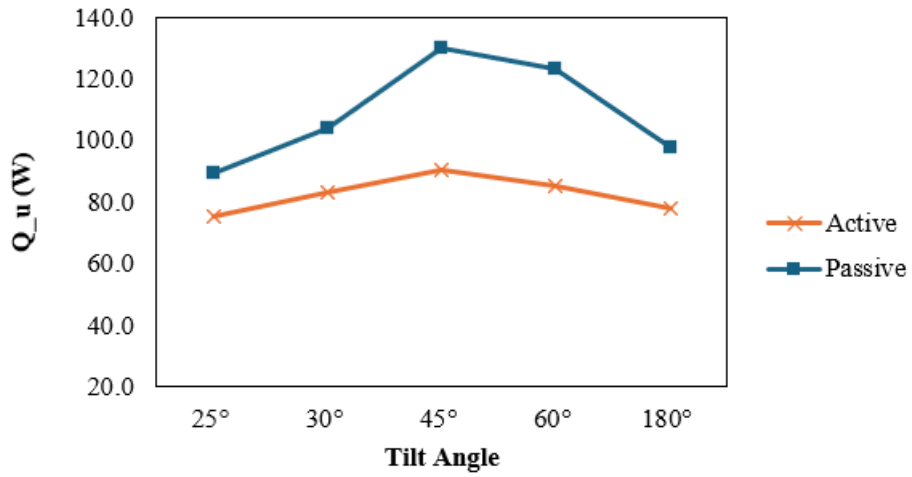

Figure 14: Useful heat gain for active and passive modes at different tilt angle

3.5.3 Effect of tilt angle on thermal efficiency

The thermal efficiency for active and passive modes at different tilt angle is given in Figure 15. The efficiency of the passive mode outperformed the active mode at all tilt angles. This may be attributed longer residence time of the air in the absorber tubes.

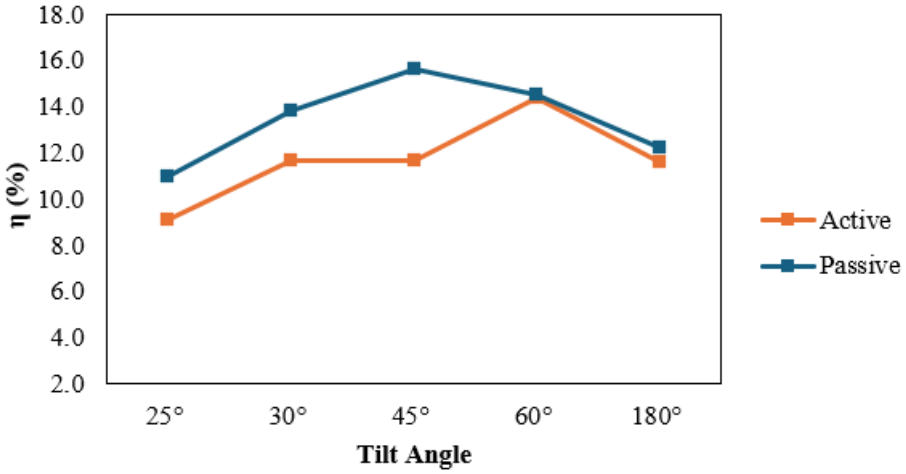

Figure 15: Thermal efficiency for active and passive modes at different tilt angle

3.6 Comparison with Literature

Table 5 compares this study's findings with previous research on low-cost solar air heaters.

Table 5: Performance Comparison with Published studies

Study	Absorber	Mode	ΔT (°C)	η (%)	Remarks
Present study	Al cans	Active	75	14	Forced convection at 0.00113 kg/s
Present study	Al cans	Passive	54	16	Optimal at 45° tilt
(Murali *et al*,.2020)	Al cans	Active	-	9-12	Lower efficiency due to different configuration
(Mgbemene *et al.*,20 22)	Al cans	Passive	-	5–8	Natural convection only

The present study demonstrates competitive performance compared to conventional designs, validating the aluminium can approach as a viable low-cost alternative. The higher efficiencies relative to some previous aluminium can studies Murali (2020) may result from improved tube configuration and optimal tilt angle selection.

3.8 Practical Implications

For active systems: The consistent performance across tilt angles suggests flexibility in installation, making them suitable for building-integrated applications where optimal orientation may be constrained. The 12 V DC fan requirement can be met with small photovoltaic panels, enabling stand-alone operation.

For passive systems: The strong tilt dependence necessitates careful orientation planning. The 45° recommendation provides design guidance for Maiduguri and similar latitudes, though seasonal adjustments could further optimize year-round performance.

4. Conclusion

This experimental investigation of a solar air heater using discarded aluminium soda cans as absorber tubes, tested under Maiduguri climatic conditions in both active and passive modes, yields the following conclusions:

Corresponding author's email address: babajidda124@gmail.com

i. Aluminium soda cans are effective low-cost absorber materials: The recycled cans achieved temperature rises of 79°C (active mode) and 54.0°C(passive mode), demonstrating thermal performance comparable to conventional absorbers at substantially reduced cost.
ii. Tilt angle significantly affects passive mode performance: Optimal passive operation occurred at 45° tilt, yielding maximum efficiency of 16%. Performance degraded at lower and higher angles, with 180° (horizontal) showing poorest results (12.2% efficiency).
iii. Maiduguri's climate is suitable for solar air heating: High irradiance levels (630–1030 W/m² during testing) enabled substantial temperature rises, confirming the region's potential for solar thermal applications.
iv. Waste-to-energy approach validated: The successful use of discarded beverage cans demonstrates a sustainable pathway combining waste management with renewable energy generation.

The study confirmed that appropriately designed aluminium-can solar air heaters offer an affordable, environmentally beneficial alternative to conventional designs, particularly suitable for resource-limited communities in solar-rich regions.

Acknowledgements

The authors acknowledge the Department of Mechanical Engineering, University of Maiduguri, for laboratory facilities and technical support.

References

Abdulkarim, BM. 2020. Performance enhancement of a single pass solar air heater by adopting wire mesh absorber layer. *Evergreen*; 10(2):880–887.

Bhowmik, H., Amin, R. 2017. Efficiency improvement of flat plate solar collector using reflector. *Energy Reports*; 3:119–123. https://doi.org/10.1016/j.egyr.2017.08.002

Incropera, FP., DeWitt, DP., Bergman, TL., and Lavine, AS. 2013. *Principles of Heat and Mass Transfer*. 7th Edition. John Wiley and Sons, USA.

Kreith, F. and Bohn, MS. 2004. *Principles of Heat Transfer*. 6th Edition. Brooks/Cole Publishing Company, USA.

Karoua, H., Moummi, A., Moummi, N., and Achouri, E. 2016. Experimentally investigated a solar air heater integrated with a Linear Fresnel Reflector (LFR). The study reported enhanced thermal performance with outlet air temperatures reaching approximately 150°C under concentrated solar radiation conditions.

Mandal, S. and Ghosh, SK. 2020. Experimental investigation of the performance of a double pass solar water heater with reflector. *Renewable Energy*; 149:631–640. https://doi.org/10.1016/j.renene.2019.11.160

Murali, A., Vasanth, S., Senthilkumar, R., and Kumar, TS. 2020. Thermal performance of a solar air heater using aluminum cans as absorbing material. Materials Today: Proceedings; 21:1667–1672.

Mgbemene, C., Jacobs, I., Okoani, A., and Ononiwu, N. 2022. Experimental investigation on the performance of aluminium soda can solar air heater. Renewable Energy; 195:182–193.

Prasad, RK., Kumar, S., and Gnanasekaran, M. A. 2017. Review of recent developments in solar air heaters. Renewable and Sustainable Energy Reviews; 77:919–939.

Sperry, G. 2011. DIY Can solar air heaters. Build It Solar Singh, S., Saini, RP., and Saini, JS. 2022. Experimental study on performance of solar air heater having multi-V-shaped roughness on absorber plate. Energy Conversion and Management; 252:115096.

Corresponding author's email address: babajidda124@gmail.com